On the development and functional roles of the horizontal connections within the primary visual cortex (V1)

Baran Çürüklü[1], Anders Lansner[2]
[1]*Department of Computer Science and Engineering, Mälardalen University, SE-72123 Västerås, Sweden*
[2]*Department of Numerical Analysis and Computer Science, Royal Institute of Technology, SE-10044 Stockholm, Sweden*

Abstract

A laminar V1 model consisting of layers 4 and 2/3 is presented. The model is in line with the modular structure of the neocortex and addresses development of the horizontal connections within the V1. Later, the functional roles of the horizontal connections are addressed. Layer 4 model exhibits sharp orientation selectivity despite poorly tuned LGN input. Sharp orientation selectivity is achieved through (i) control of the total activity of the modeled hypercolumns by normalization inhibition, and (ii) providing layer 4 units with information from a larger region than their classical receptive fields. This laminar V1 model addresses configuration-specific facilitation phenomena as well. Elongated layer 2/3 summation pools demonstrate that collinearly configured stimuli are easier to detect than orthogonally (or circularly) configured stimuli.

1 Introduction

Neurons found in the V1 respond selectively to the orientations of the bar-like stimuli (Hubel and Wiesel, 1962), whereas retinal ganglion cells and neurons that populate the lateral geniculate nucleus (LGN) prefer small point-like stimuli (Kuffler, 1953; Kaplan and Shapley, 1982). Since its discovery, the orientation selectivity (OS) property of the V1 neurons has drawn much attention (Das, 1996; Sompolinsky and Shapley, 1997; Ferster and Miller 2000; Martin, 2002). It is hypothesized that emergence of this property demonstrates how the incoming sensory information is represented by the neocortex.

In cat V1, OS is evident already in the simple cell dominated layer 4, which is the main recipient of the thalamic input (Hubel and Wiesel, 1962). According to the Hubel-Wiesel model, which is the earliest model of the OS, the receptive fields (RF) of simple cells are composed of alternated ON (light preferring) and OFF (light preferring) subfields (Hubel and Wiesel, 1962). The Hubel-Wiesel model assumes that ON subregions of the simple cells emerge through projections of the ON-center

LGN cells. OFF subregions of these neurons emerge similarly, i.e. through the projections that originate from the OFF-center LGN cells. This model assumes that the RF are strongly elongated along the axis that coincides with the simple cells' preferred orientations. According to this assumption an elongated region of the visual field is covered by the RF of the LGN cells that project to a simple cell's subfield. Thus, the anisotropy seen in the subfields is explained solely by the projections from the LGN. The Hubel-Wiesel model addresses emergence of OS in layer 4 of cat V1 in a pure feedforward fashion without and involvement of the intracortical connections.

Recently, emergence of OS (and contrast-invariance of orientation tuning) has been addressed by a more complex feedforward model (Troyer et al., 1998; Kayser and Miller, 2002; Lauritzen and Miller, 2003), which assumes opponent inhibition (Ferster, 1988). Like the Hubel-Wiesel model the opponent inhibition model assumes that the LGN input is well tuned for orientation. It also assumes that the LGN input has an additional component, which depends solely on stimulus contrast (Troyer et al., 2002). According to the opponent inhibition model a network that comprises two functionally distinct (simple and complex) inhibitory sources (Ferster, 1988; Hirsch et al., 2000; 2003) explains sharpening of the (already well tuned) LGN input, and the silencing of the component of the LGN input, which depends solely on the stimulus contrast (Lauritzen and Miller, 2003).

A number of studies have shown that the subfields of the simple cells are indeed elongated in several species, e.g. cats (Jones and Palmer, 1987; Pei et al., 1994; Reid and Alonso, 1995), and ferrets (Chapman et al., 1991). Jones and Palmer (1987) report that mean width-to-length aspect ratio of a simple cell RF having two subfields is roughly 1:1.5. These results support the existence of a thalamocortical circuitry, which is assumed by the feedforward models. However, reported aspect ratio values of the full RF, and individual subfields cannot explain sharp tuning, which is demonstrated by the V1 neurons. Orban (1984) has shown that in average simple cells respond selectively to a narrow band of orientations, i.e. ~20º at half-width at half-height. This requires stronger anisotropy in the RF than the reported values.

An essential support for the feedforward models is the cooling experiment conducted by Ferster et al. (1996). In this work the activity of the V1 neurons is reduced by cooling down the cortex to ~9ºC. During the experiment LGN is intact, and hence is the main source of input of the V1 neurons. The authors show that despite the cooling procedure V1 neurons are orientation selective. However, this support is only qualitative, since as a result of the cooling procedure the V1 neurons respond selectively to an orientation band of ~45º (half-width at half-height), which is considerably broader than the reported values (Orban, 1984). Furthermore, as pointed out by Sompolinsky and Shapley (1997), in Ferster et al. (1996) only the first harmonic of the responses are used when the tuning curve is calculated, and hence responses that are untuned for orientation are ignored. Based on these findings, Sompolinsky and Shapley (1997) argue that the results of Ferster et al. (1996) indicate that the simple cell RF have low aspect ratios. Thus, it is plausible to

assume that the emergence of OS cannot be explained solely by the thalamocortical circuitry.

An alternative approach to address the emergence of OS is taken by the recurrent models (Ben-Yishai et al., 1995; 1997; Somers et al., 1995; 2002; McLaughin et al., 2000; Wielaard et al., 2001). In contrast to the feedforward models, these models assume that the LGN input is poorly tuned for orientation. This assumption is in line with results on mildly elongated RF. Based on this assumption the recurrent models demonstrate that sharp orientation tuning emergences mainly through lateral interactions mediated by the horizontal connections. Recurrent models assume that the result of the lateral interactions is the manifestation of the so-called Mexican Hat activity pattern, which guarantees that the neuron activities are considerably higher in the center of this active region than in the surroundings. However, the recurrent models achieve the Mexican Hat activity pattern either by an odd arrangement of the horizontal connections (Ben-Yishai et al., 1995; 1997; Somers et al., 1995; 2002) or by extremely strong inhibition (McLaughin et al., 2000; Wielaard et al., 2001) (see Martin (2002) for a critical review of feedforward and recurrent models of hypercolumns).

According to the connection pattern proposed in Ben-Yishai et al. (1995; 1997) and Somers et al. (1995; 2002) inhibitory connections extend longer than their excitatory counterparts. Narrowly tuned excitatory input in combination with broadly tuned inhibition generates effectively the desired Mexican Hat activity pattern. However, as also pointed out in Martin (2002), the connection pattern in layers 4 and 2/3 of the V1 is the opposite (Ferster, 1988; Kritzer et al., 1992; McDonald CT and Burkhalter 1993; Kisvárday et al., 1997; Hirsch et al., 2000; 2003; Roerig and Chen, 2002). Kisvárday et al. (1997) report that the inhibitory network is <50% of the excitatory network.

The influence of the horizontal connections over the response properties of the neurons extends beyond emergence of fundamental response properties, such as OS. There are evidences on (facilitative and suppressive) surround effects, which cannot be explained by the classical receptive fields (CRF) (Allman et al., 1985). It has been reported that the visibility of a grating stimulus improves when its size increases (Howell and Hess, 1978; Robson and Graham, 1981). Later, is has been shown that this visibility is closely related to stimulus configuration as well (Polat and Sagi, 1993; 1994a; 1994b; Polat and Norcia, 1998; Polat and Tyler, 1999; Chisum et al., 2003).

Polat and Norcia (1998) have addressed configuration-specific facilitation phenomena in human vision in low-contrast conditions. Authors propose that these phenomena reveal the non-linear interactions (summation in this case) between CRF and their non-linear surrounds. Based on measurements of visually evoked potentials in human visual cortex, the authors have shown that elongation of a foveally viewed circular Gabor patch has a positive effect on its visibility. Furthermore, elongation along the orientation axis (collinear configuration) results in a more prominent improvement in visibility than orthogonal elongation of the stimuli. Polat and Norcia (1998) propose that elongated summation pools, which

probably emerge through long-range interactions, can explain phenomena related to configuration-specific facilitation.

Long-range horizontal connections have been found in a variety of species including tree shrew (Rockland and Lund, 1982; Fitzpatrick, 1996; Bosking et al., 1997; Chisum et al., 2003), ferret (Rockland, 1985; Durack and Katz, 1996), cat (Gilbert and Wiesel, 1983; 1989; Kisvárday et al., 1997; Schmidt et al., 1997; Yousef et al., 1999), and monkey (Rockland and Lund, 1983; Amir, 1993; Malach et al., 1993). These connections, which mainly arise from layer 2/3 pyramidal and spiny stellate cells, travel up to 4 mm on (cat) cortex surface and target mainly distal iso-orientation domains (referred to as modular specificity). Since an iso-orientation domain represents roughly 1/3 of the orientations these projections become also patchy. Furthermore, these connections terminate in a region that is elongated along the orientation axis of the source neurons (referred to as axial specificity).

A recent study shows that neurons, in layer 2/3 of tree shrew V1, have elongated RF, and are sharply tuned for orientation (Chisum et al., 2003). In addition, they perform length summation, which indicates that these neurons can integrate information from remote locations. Chisum et al. (2003) have shown that along the orientation axis of the neurons the size of these summations pools coincides well with the region covered by the layer 2/3 long-range horizontal connections. Furthermore, responses to the collinearly positioned Gabor patches are stronger than responses to noncollinear constellations of Gabor patches. This result is interpreted as an indication of the axial specificity of the layer 2/3 long-range horizontal connections. According to Chisum et al. (2003) anatomical differences between layer 4 and layer 2/3 horizontal connections is reflected in the response properties of the neurons that populate these two layers. Layer 4 neurons lack far-reaching horizontal connections, which are common in layer 2/3 (Chisum et al., 2003). These neurons are also poorly tuned for orientation (Humphrey and Norton, 1980; Chisum et al., 2003), and do not exhibit length summation (Chisum et al., 2003).

It is not clear how and when the orientation map and the horizontal connections develop and take their final form. However, there seems to be a consensus on that the neurons respond selectively to stimulus orientation already at eye opening. This finding has been demonstrated on newborn kittens (Hubel and Wiesel, 1962; 1963; Blakemore and Van Sluyters, 1975; Buisseret and Imbert, 1976; Frégnac and Imbert, 1978; Albus and Wolf, 1984; Gödecke et al., 1997; Crair et al., 1998), ferrets (Chapman and Stryker, 1993; Chapman et al., 1996), and monkeys (Wiesel and Hubel, 1974). However, as pointed out in Chapman and Stryker (1993), reported values on the degree of orientation selectivity at the eye opening vary, even within the same species (in this case the cat). According to Hubel and Wiesel (1963) all neurons are orientation selective already at eye opening, whereas others are more conservative and suggest that 25–30% of the neurons respond selectively to stimulus orientation (Blakemore and Van Sluyters, 1975; Buisseret and Imbert, 1976; Frégnac and Imbert, 1978; Albus and Wolf, 1984).

It has also been reported that the overall shape of the orientation map remains unchanged when the newly opened eyes are subject to normal visual experience (Chapman et al., 1996; Crair et al., 1998; White et al., 2001). Thus, it seems that the

genetic factors play an important role in the emergence of the orientation map, whereas the impact of the visual experience on this process is unclear (Gödecke et al., 1997; Crair et al., 1998; Chapman et al., 1999; Miller et al., 1999). However, after eye opening the neurons' selectivity to orientations increases significantly (Blakemore and Van Sluyters, 1975; Frégnac and Imbert, 1978; Chapman and Stryker, 1993; Chapman et al., 1996; Gödecke et al., 1997; Crair et al., 1998; White et al. 2001). Furthermore, this period coincides with the maturation of the horizontal connections. Note also that dark rearing or binocular deprivation can alter normal development of the orientation map, as well as the horizontal connections (Imbert and Buisseret, 1975; Chapman and Stryker, 1993; Chapman et al., 1996; White et al., 2001). These studies indicate that the orientation map continues to develop after the eye opening, and takes its final form through the interactions mediated by the developing thalamocortical circuitry, and the horizontal connections.

It is hypothesized that the layout of the horizontal connections plays an important role in the emergence of OS, and the manifestation of configuration-specific facilitation phenomena. To address these issues a laminar model of the V1 is proposed and examined here.

2 Methods

2.1 Model overview

The model consists of layers 4 and 2/3 of V1 as well as the thalamic input to V1. Each modeled cortical layer is a Bayesian Confidence Propagation Neural Network (BCPNN) (Lansner and Ekeberg, 1987; 1989; Lansner and Holst, 1996; Holst, 1997; Sandberg et al., 2002; Sandberg, 2003). Modeled cortical layers are connected to each other in a feedforward manner (see Fig. 11.1 and Section 11.5.2). Consequently, information flow between the components of the model is LGN → layer 4 (BCPNN) → layer 2/3 (BCPNN). Layer 2/3 does not receive direct LGN input (Fig. 11.1).

The LGN is not modeled explicitly. Instead, input to V1 is calculated based on a simplified but realistic model of the thalamic input to the cortical neurons. The LGN cell response model proposed by Troyer et al. (2002) has been modified and extended to fit the proposed model (see Section 11.5.1).

The experiments consist of two distinct studies. In the first study, emergence of OS within the layer 4 is addressed. Later, configuration-specific facilitation phenomena in layer 2/3 are addressed. These studies aim to illustrate the influence of the fully developed horizontal connections on the manifestation of these two phenomena. Each study starts with the learning phase, during which the horizontal connections are developed. Network behavior is investigated in the retrieval phase. For simplicity the feedforward path (LGN → layer 4 → layer 2/3) is assumed to be non-plastic. Note however that we do not rule out the putative influence of the postnatal development of the thalamocortical circuitry, and the interlaminar connections on the manifestation of these phenomena, especially emergence of OS.

2.2 LGN input to V1

Modeled LGN input has two components (Troyer et al., 2002). The first component is a function of both stimulus orientation and stimulus contrast (Eq. 11.2). The second component is untuned for stimulus orientation, i.e. it is solely a function of stimulus contrast.

Since the V1 model addresses interactions near fovea, it is assumed that the LGN X cells are the main source of sensory input (Ferster, 1990). These cells have roughly linear contrast gain functions (Derrington and Lennie, 1984). Consequently, it is assumed that the LGN input is a linear function of the stimulus contrast (Eqs. 11.4–11.6).

In the model the LGN input is poorly tuned for orientation (Eq. 11.1). The half-width of the tuning curve at half-height is 47.2º. This value is in line with reported values on low RF aspect ratios. The LGN input is also considered to be weak, despite the indications that the LGN EPSPs have higher amplitudes than the intracortical EPSPs (Stratford et al., 1996). Weak LGN input is in line with the finding that most synapses in layer 4, which is the main recipient layer of the thalamic input to the cortex, are of cortical origin. Among the synapses that target a layer 4 neuron, between ~4% (Garey and Powell, 1971; Hornung and Garey, 1981; Winfield and Powell, 1983; LeVay, 1986; Peters and Payne, 1993; Ahmed et al., 1994), and ~24% (LeVay and Gilbert, 1976; Einstein et al., 1987) originate from the LGN. In the model it is assume that 2/3 of the excitatory drive originate from layer 4, whereas 1/3 originate from the LGN input ($\Psi_{L4} = 2/3$, see Section 11.5.2).

2.3 V1 model

The modular structure of the neocortex has been the primary influence of the BCPNN (Mountcastle, 1957; 1978; 1997; Powell and Mountcastle, 1959; Hubel and Wiesel, 1962; 1977; Buxhoeveden and Casanova, 2002). Thus, a BCPNN consists of modules that are abstractions of hypercolumns (referred to as 'hypercolumn-modules' in the text). These hypercolumn-modules consist of units that correspond to cortical minicolumns (orientation minicolumns in the context of this paper). Activity of a unit is the mean firing rate of the population of neurons that the unit represents.

Each BCPNN comprises 49 (7x7) hypercolumn-modules, arranged to form a hexagonal array. The diameter of a hypercolumn-module is 1 mm (Kisvárday et al., 1997). The center-to-center distance in visual angle between two adjacent hypercolumn-modules is 1/(√3)º (~0.58º). Along the horizontal axis the distance between two adjacent hypercolumn-modules is 0.5º. The center-to-center distance, and hence the cortical magnification factor, is fixed throughout the network model.

The layer 4 hypercolumn-modules consist of 12 units, whereas their layer 2/3 counterparts comprise six units. The RF centers of the units are positioned in the center of their so-called host hypercolumn-modules. The RF of the layer 4 units are modeled as contrast edge detectors (Section 11.5.1). These units are tuned for the spatial frequency of 1 c/deg. For the simplicity all RF widths are 1º. Thus, there is a substantial overlap between units positioned in adjacent hypercolumn-modules. The

difference in orientation preference between two successive layer 4 units inside a hypercolumn-module is 30º. Note that two units represent one orientation when the signs of their RF subfields are ignored. The RF of these two units have opposite absolute spatial phase relative to each other. There are six such anti-phase unit pairs in each layer 4 hypercolumn-module. Each layer 2/3 unit receives input from an anti-phase pair located in the layer 4 hypercolumn-module below (Eq. 11.7). As a result, complex cell like RF of layer 2/3 units are generated. Only 10% of the excitatory drive of a layer 2/3 unit is from the layer 4 anti-phase pairs ($\Psi_{L23} = 0.1$). This ratio is in line with the finding that in layer 2/3 the main part of the input is from other layer 2/3 neurons.

The total activity within a hypercolumn-module is normalized to one (Eq. 11.8). This procedure is supported by the studies on response saturation phenomena of the V1 neurons (Maffei et al., 1973; Dean, 1981; Albrecht and Hamilton, 1982). Albrecht and Hamilton (1982) have shown that, as stimulus contrast increases, the neurons increase their activities up to the level of ~50–60% of their maximum response levels (determined by their electrical properties). This behavior is followed by rapid saturation and normalization. In the normalization phase the neurons have roughly constant responses, i.e. they do not increase their activities due to increase in stimulus contrast. It is thus hypothesized that mechanisms behind the normalization phenomenon play an important role in keeping the total activity within a cortical patch under a certain level.

Similar to the cortex, in the BCPNN normalization aims to limit the maximum activity. In the V1 model normalization is carried out simply by dividing the activities of the units with the total activity of their host hypercolumn-modules (Eq. 11.8). Observe that this procedure is purely mathematical. The detailed neuronal mechanisms have been addressed earlier in the cortical hypercolumn model derived from the BCPNN architecture (Çürüklü and Lansner, 2002). One important assumption was made on the linear response of the LGN cells to contrast stimulus increase (Derrington and Lennie, 1984). Thus, rapid saturation followed by normalization was explained solely by interactions within the model. One inhibitory neuron integrated the activity of the input layer excitatory neurons, and inhibited excitatory neurons found in the output layer (referred to as the normalization inhibition). This single inhibitory neuron represented a population of inhibitory neurons evenly distributed in a cortical hypercolumn. Since this inhibition become mainly a function of the stimulus contrast, its tuning relative excitatory inputs become less significant then in other recurrent models (Ben-Yishai et al., 1995; 1997; Somers et al., 1995; 2002). Such an inhibition can be mediated by a combination of inhibitory complex and simple cells (Hirsch et al., 2000; 2003; Krimer and Goldman-Rakic, 2001; see Section 11.5.2 for the details).

The BCPNN learning algorithm is correlation based, and hence if two units are correlated in a time step the connection between them strengthens (Eqs. 11.9–11.13). Anti-correlation results in development of an inhibitory connection via local inhibitory interneurons (Ferster, 1988; Hirsch et al., 2000; 2003). As a consequence, horizontal connections in the V1 model run between two units, and represent groups

of excitatory axons that originate from one orientation minicolumn and target either excitatory or inhibitory neurons in the target orientation minicolumn (these connections are referred to as E→E and E→I connections, respectively).

In layer 4 of cat, inhibitory simple cells inhibit excitatory simple cells that are located in their close surroundings if they have opposite absolute spatial phase relative their excitatory targets, i.e. their subfields with opposite sign overlap (Ferster, 1988). Absolute spatial phase refers to the position of the ON- and OFF-subregions with respect to the visual field. Based on Ferster (1988) it is hypothesized that anti-correlated units can inhibit each other by local or long-range E→I connections. In the BCPNN model this inhibition is implemented by a non-plastic inhibitory connection. Strength of this non-plastic connection is one, and hence the strength of the inhibition is given by the E→I connections. In contradiction to the normalization inhibition, latter form of inhibition is highly selective and connects anti-correlated units to each other. Thus, these two forms of inhibition have both different connectivity patterns, and functional roles.

Learning phase corresponds to the period that follows eye opening and continues for roughly four weeks (Crair et al., 1998; White et al., 2001). During this critical period the development of the cortex can be altered by visual deprivation. The learning phase is 10000 simulation time steps long. During each time step a new contrast edge stimulus is generated. Since the learning phase corresponds to a rather vague time period the learning time step is dimensionless, and is set to one. The network's learning capacity depends on the dimensionless learning rate $\alpha = 0.05$, which is the inverse of the learning time constant τ_L (Eqs. 11.9–11.13).

Position, orientation ($0^o \leq \theta_{st} < 360^o$), and contrast ($0 \leq c \leq 1$) of the contrast edge stimuli are sampled from a uniform distribution. Their spatial frequency is 1 c/deg, width is 1º, and they are infinitely long. It is assumed that these contrast edge stimuli correspond to small fractions of real images, and hence mimic natural visual images seen by a small patch of the V1. After adding Gaussian noise with standard deviation of 5% to the units' activity values, correlations between pairs of units in each layer are calculated. Based on the degree of correlation weights and biases are updated. Thus, the weight matrix reflects the degree of correlation between unit pairs.

Retrieval time step as well as the membrane time constant (τ_C) of the units are 2 ms. Gaussian noise with standard deviation of 2.5% is added to LGN input before it is fed into the units, whereas the intracortical input is modified with a Gaussian noise with standard deviation of 5%. In the OS study the model is tested on detection of contrast edges. In the second study the stimuli are sinusoidal gratings.

To see if the V1 model has detected the stimuli the units that are located in the center hypercolumn-modules are monitored (they are positioned in the center of the 7x7 network model (Fig. 11.2)). In the OS study center hypercolumn-module of the layer 4 is monitored, whereas in the second study its layer 2/3 counterpart is monitored. Since the BCPNNs are configured as attractor networks, the monitored center hypercolumn-module will converge to an orientation, which is represented by a unit (this applies to all other hypercolumn-modules as well). If the orientation

preferences of that unit and the stimulus are same, it is assumed that the V1 model has detected the stimulus (in the text the unit, which represents the orientation of the stimulus, is referred to as the reference unit). However, if the center hypercolumn-module has converged towards another orientation the stimulus has not been detected.

A simulation continues until an orientation has been detected, or if this does not occur the simulation is terminated after 200 ms. This time period is considered to be sufficient for a convergence to occur. By definition, convergence occurs when the following three requirements are fulfilled simultaneously in the monitored center hypercolumn-module: (i) any unit's activity is >0.75 (recall that the total activity is 1 in a hypercolumn-module), (ii) between two consecutive time steps mean difference in activity for the units is <0.1, and (iii) requirements (i–ii) must be valid for a time period of 20 ms.

Simulation results are evaluated quantitatively by measuring confidence in convergence, and mean convergence times. Confidence is the number of correct detections divided by the number of trials for each simulation setting. High confidence means sharp tuning. The second measurement is the mean time for correct convergences, for each simulation setting. The 20 ms time period, which is required for testing convergence, is not included in the convergence time.

3 Results

Emergence of OS within the layer 4

In this work it is hypothesized that there is a strong correlation between the lateral extent of the layer 4 network, and the degree of OS demonstrated by the V1 neurons. To investigate the validity of this hypothesis a V1 model has been trained. Later, with respect to the lateral extent of the layer 4 network two V1 models are configured. These two networks inherit the properties of the original layer 4 network as well as allow an examination of our hypothesis. In this study the layer 2/3 component of the V1 model is ignored.

In the first of these two network configurations, solely horizontal connections within a hypercolumn-module are permitted, and hence this network is referred to as the 'local network'. In the second configuration connections between adjacent hypercolumn-modules are also allowed (Fig. 11.2). This network is referred to as the 'full network'. Lateral extent of the full network corresponds to the distance traveled by most excitatory axons, i.e. less than 2 mm (Yousef et al., 1999). The hypothesis is that the full network units are more orientation selective than their local network counterparts, since they have access to information from a larger region of the visual field. It is assumed that this hypothesis is in line with what is found in the V1. In monkey, layer 4Cβ cells are not selective to orientation, in contrast to the layer 4Cα neurons (Hubel and Wiesel, 1977; Blasdel and Fitzpatrick, 1984; Hawken and Parker, 1984). One possible explanation for this finding might be that the lateral connections in layer 4Cα are more prominent than those found in layer 4Cβ (Martin, 2002). Cat layer 4 neurons are orientation selective (Hubel and Wiesel, 1962). These neurons have widespread lateral connections (Martin and Whitteridge, 1984; Yousef

et al., 1999). Note also that layer 4 neurons in tree shrew (Humphrey and Norton, 1980; Chisum et al., 2003), and ferret (Chapman and Stryker, 1993) are poorly tuned for orientation, whereas their counterparts in layer 2/3 demonstrate sharp tuning. Since the LGN afferents rarely target layer 2/3 (Bullier and Henry, 1979; Ferster and Lindstrom, 1983; Martin and Whitteridge, 1984), it is plausible to assume that the layer 2/3 horizontal connections play an active role in the emergence of OS in these species.

For a valid comparison of the local and full networks all four sources of inputs (local and long-range excitatory/inhibitory) are modified to have the same amplitude. This is achieved by minor modifications of the original layer 4 weight matrix. Now, by having different layer 4 internal gains, total strength of a unit's input can be controlled (independently of network configuration). In the local network configuration the internal gain is double that of full network to compensate the missing long-range connections (γ_h^{L4} in Section 11.5.2 is 90 and 45 respectively). The gain of the LGN input source is the same for both configurations: $\gamma_{ext}^{L4} = 90$. Layer 2/3 gains are 90 throughout the simulations. It is important to point out that despite weight modification and limiting the lateral extent of the horizontal connections quantitative properties as well as behavior of the original layer 4 network are preserved in the full network, since in the original network long-range inputs (excitatory and inhibitory) are as strong as the local inputs, and inhibition is roughly the half of the excitation.

Based on the full network quantitative assessments of the horizontal connections have been done (Tables 11.1 and 11.2). This helps to classify layer 4 connections in three groups; iso- (±30º), oblique- (±30–60º), and cross-orientation (±60–90º), and hence reveal the degree of correlation between these three orientation domains. First, projections that involve the reference unit are classified (Fig. 11.3*A*). Later, a population, with the reference unit in the core, has been put together. It is assumed that this population represents a small cortical patch, which corresponds to an injection site (Fig. 11.3*B*). Observe that the horizontal connections are reciprocal, and hence Tables 11.1 and 11.2 can be interpreted both as inputs and outputs of these two hypothetical patches.

It is evident that in the both cases local and long-range E→E connections prefer the iso-orientation domain (Tables 11.1 and 11.2). Still, ~50–60% of the E→E connections are between oblique- and cross-orientation domains. Local E→I connections do show the same projection pattern as the E→E connections. Observe that strongest inhibition is at iso-orientation (Ferster, 1986; 1988). Furthermore, due to uncorrelated inputs direct cross-orientation inhibition is very weak. The model explains cross-orientation inhibition (Morrone et al., 1982; Bonds, 1989) by normalization inhibition, since this form of inhibition integrates total activity of a hypercolumn-module and inhibits all units equally strong (Çürüklü and Lansner, 2002). The result is net inhibition for those units that are not selective for the stimulus. Long-range E→I connections target mainly the cross-orientation domains (Tables 11.1 and 11.2). When two connection types are combined, the long-range connections become equally distributed between the three orientation domains.

These results are relatively independent of parameter settings. When the lateral extent increases long-range E→E as well as E→I connections become even less selective. Thus, the total effect is unaffected. Due to increase in network size units see the stimulus more seldom. The result is reduced weight amplitudes. Connection patterns are not influencing though. The only parameter that has a major influence on the results is center-to-center distance in visual angle. When this parameter decreases hypercolumn-modules start to collapse to one spot in the visual field. As a result all distributions become as in the local connection case. Note that changing the center-to-center distance does also affect the pattern of long-range connections. Based on the degree of correlation between unit pairs these connections can be inhibitory or excitatory. This does not affect the numbers presented in quantitative assessments though. Furthermore, results in Tables 11.1 and 11.2 are representative for other orientations as well. Since the (hexagonal shaped) network is not symmetric in all directions (and to examine if corner effects influence the results) quantitative assessments for units with preferred orientations 0º, 30º, and 60º have been done. The results were similar to those presented in Tables 11.1 and 11.2. Taken together, the quantitative assessments of the full network suggest that local connections prefer the iso-orientation domain, whereas long-range connections are distributed equally between orientation domains. This result is in agreement with the quantitative assessment of the layer 4 (Yousef et al., 1999).

In the retrieval phase mechanisms behind OS is investigated by analyzing network performance on detection of vertical contrast edge stimuli ($\theta_{st} = 90°$), in high- and low-contrast conditions (50 and 5%, respectively). The stimuli are positioned at the middle hypercolumn-module. Their spatial frequencies and widths are 1 c/deg and 1º, respectively. In order to investigate robustness of the results, and also demonstrate how the horizontal connections influence OS, excitatory (E→E) and inhibitory (E→I) strengths are varied (step length = 1), for each network configuration and contrast. For each such combination, simulations are repeated 100 times. Since the local network behavior is found to be highly unpredictable, and almost impossible to quantify (with respect to confidence as a function of connection strengths) 200 such simulation series have been done. One such simulation series is shown here (Figs. 11.4 and 11.5). Some 50 additional simulations have been done to verify that the results presented in Figs. 11.4 and 11.5 are representative for all orientations (as previously, these orientations were 0º, 30º, and 60º).

Roughly one fourth of the trained local networks behaved as in Figs. 11.4*C–D*, however, with considerably lower maximum confidence values in the most of the cases (and never higher than their full network counterparts). OS was practically absence, i.e. <0.08, in the remaining local networks, independent of connection strengths and stimulus contrast. Observe that in absence of stimulus monitored hypercolumn-module can converge to any of the 12 orientations, and hence the threshold of correct detection is ~0.08. Lower confidence values indicate no convergence within the 200 ms time period (Fig. 11.4). Increase of time period (in

this case to 500 ms) does not change the results, and hence it is assumed that in general local network performance with respect to OS is poor and unpredictable.

There are major differences between the behavior of the full and local networks. In both contrast conditions full network can detect the stimuli (Figs. 11.4*A–B*), whereas the performance of the local network is considerable poorer, especially when excitation is increased (Figs. 11.4*C–D*). Remember also that this layer 4 network performs better than most of the trained layer 4 networks.

The full network confidence graphs reveal that the horizontal connections play an important role in the emergence of OS (Figs. 11.4*A–B*). When the E→E connections are absent the full network performs poorly. Even when inhibition is absent, i.e. both connection strengths are set to zero, converge within the given time period is not possible. Note that this case corresponds to the situation right at the beginning of the learning phase, since horizontal connections are absent. It is thus assumed that for the proposed layer 4 model, i.e. the full network, poorly tuned LGN input is not sufficient for the emergence of OS (Fig. 11.4).

Independent of network configuration and contrast highest confidence values are yield when the excitatory connections are untouched (E→E strength = 1). This finding has been verified with additional simulation, during which the connection strength step length was 0.1 (instead of one as in 11.4). Thus, the E→E weights, which are the result of training with the BCPNN learning algorithm, yield highest degree of OS.

In general, increase in E→E strength decreases the confidence values, since the probability of converging to neighboring units increases, as a consequence of increased activity (Fig. 11.4*B*). Decrease in confidence can be compensated if the E→I strength is increased as well (Fig. 11.4*B*, see also Çürüklü and Lansner (2004)). A natural consequence of increase in total excitation is also faster convergence (Fig. 11.5). For the full network when the connection strengths are untouched mean convergence times are 53.5 ms (standard deviation = 9.3 ms), and 76.8 ms (standard deviation = 19.1 ms), respectively, in high- and low-contrast conditions. Mean convergence times for the local network are considerable lower: 63.9 ms (standard deviation = 18.8 ms), and 93.2 ms (standard deviation = 23.7 ms). Thus, even if the confidence of the local network matches that of the full network, which rarely happens, it converges slower. The variations in standard deviations between network configurations indicate that the local network is less reliable even in high-contrast conditions. Furthermore, in both configurations the networks converge slower when the stimulus contrast decreases. This so-called latency shift takes roughly the form of an exponential decay function (Albrecht et al. (2001) approximate latency shift by an inverted Naka-Rushton function).

A careful analysis of Figs. 11.4 and 11.5 reveals a possible functional role of inhibition. Assume that decrease in convergence time is desired. This can only be achieved by increasing excitation (Fig. 11.5). However, a consequence of increased excitation is also decrease in confidence. The only way of tackling this problem is to increase inhibition as well. Thus, a combined increase in excitation and inhibition does speed up the network without decreasing the confidence.

Full network units have larger RF due to horizontal connections. In this context the center-to-center distance in visual angle between two adjacent hypercolumn-modules plays an important role, since performance of the full network worsens if this distance is decreased. Not surprisingly, when this distance is 0º, there are practically no differences between the full and local networks in convergence confidence (full network is somewhat more consistent in its behavior due to averaging of the inputs). Consequently, the role of these connections is not only to smooth out noisy input. This is yet another indication of that there is a correlation between network performance and lateral extent of the horizontal connections.

Configuration-specific facilitation in layer 2/3

Learning phase is carried out as in the OS study. The layer 4 network is configured as a full network with connections strengths set to one, whereas the layer 2/3 network is untouched (Fig. 11.6). Input from the layer 4 anti-phase unit pairs generates a patchy, axially specific layer 2/3 network, which is similar to layer 2/3 of the V1 (Kisvárday et al., 1997).

Presence of patches located at iso-orientation domains is an indication on correlated activity between units that are selective for similar orientations (Fig. 11.6; Tables 11.3 and 11.4). Apparently, the network does not develop E→I connections, which indicates absence of anti-correlated activity between unit pairs in layer 2/3 network. Recall that these connections are common in layer 4 network, especially between anti-phase unit pairs within a hypercolumn-module (Fig. 11.2). Quantitative assessments of the layer 2/3 reveal that 50–55% of the E→E connections are between iso-orientation domains, whereas 30–33% and 15–17% are between oblique- and cross-orientation domains, respectively (Tables 11.3 and 11.4; constellations of receiving populations correspond to those in the layer 4 cases, see Fig. 11.3). There are minor differences between local and long-range connection distributions. The former are somewhat more selective for the iso-orientation domain. These findings are further verified with quantitative assessments of units that prefer other orientations as well (0º, 30º, and 60º). These numbers are in line with what has been reported by Kisvárday et al. (1997).

The region covered by the layer 2/3 long-range horizontal connections is elongated along the orientation axis of the units. This is due to the elongated shape of the contrast edge stimuli used in the learning phase. Consequently, when these stimuli are less elongated the layer 2/3 networks become less axially specific. Unit pairs that are close to each other in space are more correlated than those far away. The result is decrease in connection strengths with increased distance. Otherwise different parameter settings generate similar network layouts, and hence it is assumed the results are robust. Especially the modular specificity is evident in all trained layer 2/3 networks.

Configuration-specific facilitation has been investigated using three different vertically orientated ($\theta_{st} = 90°$) Gabor patch stimuli (Table 11.5) under various contrast conditions (5, 10, 20, and 100%). In the first case the retrieval stimulus is a circular Gabor patch. The remaining two stimuli are elongated along one axis: either along horizontal (orthogonal configuration) or vertical (collinear configuration).

Layer 2/3 network is tested 100 times on each contrast and stimulus configuration. Only some 20 simulation series have been done since the layer 2/3 network behavior is fairly deterministic. As in the OS study confidence values are calculated. One such simulation series is shown here (Fig. 11.7). In this context confidence values reflect the degree of facilitation as a function of stimulus configuration (and contrast). High confidence means sharp OS, and hence is an indication on strong facilitation.

The result of elongation of the stimulus is increase of stimulus area. The consequence is increase of confidence independent of stimulus contrast (Fig. 11.7). This improvement in confidence is further configuration-specific, since collinear configuration results in a more prominent increase of the confidence than orthogonal. These results are in line with the studies on configuration-specific facilitation phenomena (Polat and Norcia, 1998; Chisum et al., 2003).

Differences in facilitation effects are more prominent in low-contrast (5%), since in this case ratios between confidences for circular, orthogonal, and collinear configurations are 1.0:2.0:2.7 (Fig. 11.7). This shows that in low-contrast collinearly configured stimuli are almost three times easier to detect that circularly configured stimuli. When stimulus contrast is high layer 2/3 network detects all three stimuli equally well (Fig. 11.7). In high-contrast (100%) the same ratios are 1.0:1.2:1.3. Apparently, the network is less dependent on stimulus configuration in high-contrast. Differences in facilitation between circular and collinear configurations are still evident even in high-contrast though. This result is in line with Chisum et al. (2003). Furthermore, independent of stimulus configuration, confidence increase is linear as a function of log contrast, as reported by Polat and Norcia (1998). This suggests fast improvement of confidence as a function of contrast increase in low-contrast conditions.

It is assumed that the layer 2/3 is responsible for configuration-specific facilitation phenomena. Layer 4 network is circular and mainly local (Fig. 11.2), thus behavior of this network is not likely to depend on stimulus configuration. In other words, layer 4 network cannot notice the differences between these three stimuli. The situation is different for the layer 2/3 network, since in this case units receive input from an anisotropic region (Fig. 11.6), which is overlapped with the stimulus. As a consequence, input from collinearly positioned units (with similar orientation preferences, due to modular specificity) is stronger than from all other units in the layer 2/3 network. Recall also that horizontal connections are reciprocal, thus units along the line, which overlaps with the stimulus, excite each other even more.

Since one anti-phase unit pair targets each layer 2/3 unit, low layer 4 RF ratios are preserved in layer 2/3. Thus, In the V1 model confidence-specific facilitation phenomena are not due to elongated CRF (Gilbert and Wiesel, 1985; DeAngelis et al., 1994). Neither is total amount of excitatory input is different due to stimulus configuration, since the hypercolumn-modules are normalized. Thus, in this study configuration-specific facilitation phenomena are explained solely by the axially specific layout of the long-range horizontal connections in layer 2/3.

Only one parameter did influence the simulation results considerable, i.e. center-to-center distance in visual angle between two adjacent hypercolumn-modules. When this parameter is decreased layer 4 units become less orientation specific, this has a negative effect on the confidence values in layer 2/3 as well. Nevertheless, differences in facilitation were still evident. The simulations have been done with other orientations as well (0º, 30º, and 60º) with similar results as in Fig. 11.7, thus it is assumed the precise layout of the long-range horizontal connections does not influence the results.

4 Conclusions

In this paper, a laminar model of the layers 4 and 2/3 of the V1 is presented. The model addresses development as well as functional roles of the horizontal connections found in these two cortical layers. It is assumed that both layers are subject to visual experience at the eye opening. It is further assumed that the LGN input is poorly tuned for orientations. These two assumptions are sufficient for explaining how correlation based networks of horizontal connections are developed simultaneously in modeled layers 4 and 2/3 by the BCPNN learning rule. These assumptions are in line with reports on rapid improvement of OS during the first weeks after eye opening, when the eyes are subject to normal visual experience. This period coincides with the development of the horizontal connections as well. Thus, it seems that improvement of response properties of the neurons is closely related to normal development of these connections. This process is fragile though, since manipulation of the visual input, e.g. through dark rearing or binocular deprivation, alters normal development of these connections. One indication of this is the reduction of the lateral extent of these connections.

The resulting networks resemble some of the cortical layers' properties. In layer 4 network, units that are correlated develop E→E connections, whereas anti-correlation results in the development of E→I connections. Both types of connections target mainly the local iso-orientation domain, thus iso-orientation inhibition dominates cross-orientation inhibition. The layout of the long-range connections is different though. These connections are distributed equally between orientation domains. Due to the elongated shape of the stimuli used in the learning phase the connections in layer 2/3 network become axially specific. Modular specificity in layer 2/3 is explained by the finding that units in this layer are rarely anti-correlated. Patches are located at the iso-orientation domains. This indicates strong correlated activity between units that are selective for similar orientations. It remains to be shown if the same conditions are in fact valid during the development of V1 in reality.

In both layers normalization inhibition operates within a hypercolumn-module. In layer 4 there is an additional source of inhibition mediated by the (excitatory) E→I connections. These connections target local inhibitory interneurons, thus this form of inhibition is local as well. These assumptions are in line with what is found in the V1, i.e. inhibition is mainly local, whereas excitation extends far beyond the

inhibitory network. Observe also that neither excitation nor inhibition dominates the network.

The V1 model addresses phenomena that are related to the layout of the horizontal connections. In the first study it is shown that the presence of normally developed horizontal connections is responsible for emergence of OS. This is in line with rapid improvement of this response property after eye opening. Furthermore, the simulation results suggest that this property is dependent on the lateral extent of the horizontal connections. In the full network case the units are highly orientation selective, in contrast units in the local network are poorly tuned. Recall that in both cases the units receive roughly the same amount of excitation. When the horizontal connections are absent the network cannot even converge. This indicates absence of OS.

The proposed layer 4 network addresses OS by assuming (i) normalization inhibition for controlling the total activity of the hypercolumn-modules, and (ii) long-range E→E connections, which provide units with information from a larger region than their CRF. Increase in the strengths of the E→E connections decreases convergence times as well as confidence values. The E→I connections play a major role in stabilizing the activity of the units though. Increasing the strengths of these connections prevents the drop off in confidence values without affecting convergence times. Observe the layer 4 network addresses OS by assuming V1 like connectivity, i.e. the network is not dominated by extremely strong inhibition, and the excitatory network encloses its inhibitory equivalent.

It seems that the elongated summation pools in the layer 2/3 network can address configuration-specific facilitation phenomena. Simulation results suggest that the visibility of a stimulus is improved due to its elongation along one direction. Not surprisingly the degree of facilitation, and hence improved visibility, is related to the direction of elongation, since summation pools found in the layer 2/3 network are axially specific along the orientation axis of the units. Observe that anisotropic inputs from this network are sufficient for explaining configuration-specific facilitation phenomena. It seems also that differences in facilitation effects are more prominent in low-contrast conditions. Note further that the layer 4 network receives input from a circular region, and hence does not take part in this process.

Based on these results it is plausible to assume that the horizontal connections play an important role in the formation of the V1 neurons' response properties. Our intention is to examine further issues related to development as well as functional roles of these connections.

5 Appendix

5.1 LGN input equations

Tuning curve of the LGN input is defined by the following equation:

$$\Omega_{\sigma_{os}}(\delta\theta) = e^{\frac{-\delta\theta^2}{2\sigma_{os}^2}}, \qquad (1)$$

where $\delta\theta = \theta_{st} - \theta_{rf}$ is the orientation preference difference (in radians) between the orientation of the contrast edge stimulus (θ_{st}), and the orientation preference of a unit (θ_{rf}). Parameter σ_{os} defines the sharpness of the orientation tuning. In the simulations $\sigma_{os} = 0.7$, which yields poor tuning (half-width at half-height is 47.2º).

The LGN input has two components (Troyer et al., 2002):

$$i_{LGN}(x, y, c, \delta\theta) = DC(c) + F1(c) \cdot \Omega_{\sigma_{os}}(\delta\theta) \cdot f_{\gamma_x \gamma_y \lambda_{st} \sigma_{st}}(x, y) a, \qquad (2)$$

where

$$DC(c) = F1(c) = \frac{c}{2}, \quad 0 \le c \le 1 \qquad (3)$$

and

$$f_{\gamma_x \gamma_y \lambda_{st} \sigma_{st}}(x, y) = \cos\left(\frac{2\pi \cdot x}{\lambda_{st}}\right) \cdot e^{-\frac{x^2\gamma_x^2 + y^2\gamma_y^2}{2\sigma_{st}^2}}.$$

Parameters γ_x and γ_y (together with σ_{st}) define the extent of the stimulus in x- and y-axis respectively. Spatial frequency of the stimulus is given by $1/\lambda_{st}$. Before feeding into the layer 4 units the LGN input is rectified, since the mean LGN activity cannot fall below zero:

$$I_{LGN}(x, y, c, \delta\theta) = \max[i_{LGN}(x, y, c, \delta\theta), 0].$$

5.2 V1 model equations

Standard BCPNN framework, which consists of network architecture and learning rule (Sandberg et al., 2002), has been adapted to the simulations that are done with the proposed V1 model. Following equation defines the total input ($H_{jj'}^{\xi}$) of unit *jj'*. This unit, whose orientation is represented by the index *j'*, is located in hypercolumn-module *j*, and cortical layer model ξ:

$$H_{jj'}^{\xi} = \Psi_{\xi} \gamma_h^{\xi} h_{jj'}^{\xi} + (1 - \Psi_{\xi}) \gamma_{ext}^{\xi} ext_{jj'}^{\xi}, \quad \xi \in \{L4, L2/3\}, \qquad (4)$$

where

$$0 \le \Psi_\xi \le 1,$$

(5)

and

$$\gamma_h^\xi \max\left(h_{jj'}^\xi\right) = \gamma_{ext}^\xi \max\left(ext_{jj'}^\xi\right). \quad (6)$$

Parameter Ψ_ξ relates the two sources of inputs to each other (Eqs. 11.4–11.6). These inputs are the internal input, $h_{jj'}^\xi$, and the external input, $ext_{jj'}^\xi$. Maximum values of these two sources are defined in questions 10 and 11. Assuming one-layer network, standard BCPNN equations (Sandberg et al., 2002) is given when $\Psi_\xi = 1$. Parameters γ_h^ξ and γ_{ext}^ξ are internal and external gain respectively. Layer 4 external input is:

$$ext_{jj'}^{L4} = I_{LGN}\left(x, y, c, \delta\theta\right).$$

In the OS study two network configurations has been used for the layer 4 model. The local network configuration is obtained by (h_{ref}^{L4} is the internal input of the reference unit in layer 4):

$$\gamma_h^\xi = \gamma_{ext}^\xi, \quad -\mu \le h_{jj'}^{L4} \le \mu, \quad 0 \le ext_{jj'}^{L4} \le \mu, \quad \mu = \max\left(h_{ref}^{L4}\right),$$

and the full network configuration is obtained similarly:

$$\gamma_h^\xi = \frac{\gamma_{ext}^\xi}{2}, \quad -\mu \le h_{jj'}^{L4} \le \mu, \quad 0 \le ext_{jj'}^{L4} \le \frac{\mu}{2}, \quad \mu = \max\left(h_{ref}^{L4}\right).$$

The external input to a layer 2/3 unit is the summed activity of the two anti-phase pairs located in the layer 4 model below:

$$ext_{jj'}^{L2/3} = \hat{\pi}_{jj'}^{L4} + \hat{\pi}_{jk'}^{L4}, \quad j' \mapsto \phi, k' \mapsto \phi + 180^\circ, \quad (7)$$

$$\gamma_h = \gamma_{ext}, \quad 0 \le h_{jj'}^{L2/3} \le \mu, \quad 0 \le ext_{jj'}^{L2/3} \le \mu, \quad \mu = \max\left(h_{ref}^{L2/3}\right).$$

Internal input of unit *jj'* is defined according to the standard BCPNN equations (Sandberg et al., 2002) (index ξ is ignored for clarity in equations below):

$$h_{jj'} = \beta_{jj'} + \sum_{i}^{N} \log\left(\sum_{i'}^{M_i} w_{ii'jj'} P_{X_i}(x_{ii'}) \right).$$

The bias of unit *jj'* is:

$$\beta_{jj'} = \log(P(y_{jj'})),$$

and the weight that connects the 'presynaptic' unit *ii'* to unit *jj'* is:

$$w_{ii'jj'} = \frac{P(x_{ii'}, y_{jj'})}{P(x_{ii'})P(y_{jj'})}.$$

Convergence to the attractor state is defined through the following equation:

$$\tau_c \frac{dh_{jj'}(t)}{dt} = \beta_{jj'}(t) + \sum_{i}^{N} \log\left(\sum_{i'}^{M_i} w_{ii'jj'} f(h_{ii'}(t)) \right) - h_{jj'}(t),$$

where τ_c is 'membrane time constant' of units. The inner sum above denotes input from one of *N* hypercolumn-modules in the network.

At the end of each retrieval step the total activity within a hypercolumn-module is normalized to one (Eq. 11.8). By doing this, the total activity within the hypercolumn-modules, and consequently the network is controlled:

$$\hat{\pi}_{jj'} = f(H^{\xi}_{jj'}) = \frac{e^{H^{\xi}_{jj'}}}{\sum_{j'} e^{H^{\xi}_{jj'}}}. \tag{8}$$

In learning mode units receive solely external input. Weights and biases are updated through following equations:

$$\hat{\pi}_{ii'} = ext^{\xi}_{ii'} \tag{9}$$

$$\frac{d\Lambda_{ii'}(t)}{dt} = \alpha([(1-\lambda_0)\hat{\pi}_{ii'}(t) + \lambda_0] - \Lambda_{ii'}(t)) \tag{10}$$

$$\frac{d\Lambda_{ii'jj'}(t)}{dt} = \alpha([(1-\lambda_0^2)\hat{\pi}_{ii'}(t)\hat{\pi}_{jj'}(t) + \lambda_0^2] - \Lambda_{ii'jj'}(t)) \tag{11}$$

$$\beta_{ii'}(t) = \log(\Lambda_{ii'}(t) + \lambda_0) \tag{12}$$

$$w_{ii'jj'}(t) = \frac{\Lambda_{ii'jj'}(t)}{\Lambda_{ii'}(t)\Lambda_{jj'}(t)} \tag{13}$$

To avoid logarithmic zero $\lambda_0 = 10^{-8}$ is introduced. This parameter mimics the background activity as well. Parameter α is defined as the inverse of the learning time constant τ_L. Plasticity is induces when $\alpha > 0$, (network is non-plastic if $\alpha = 0$.

Acknowledgements

This work was supported by CUGS (the Swedish National Graduate School in Computer Science).

References

Ahmed BA, Anderson JC, Douglas RJ, Martin KA, Nelson JC (1994) Polyneural innervation of spiny stellate neurons in cat visual cortex. J. Comp. Neurol. 341:39–49.

Albrecht DG, Hamilton DB (1982) Striate cortex of monkey and cat: contrast response function. J. Neurophysiol. 48:217–237.

Albrecht DG, Geisler WS, Frazor RA, Crane AM (2001) Visual cortex neurons of monkey and cats: temporal dynamics of the contrast response function. J. Neurophysiol. 88:888–913.

Albus K, Wolf K (1984) Early postnatal development of neuronal function in the kitten's visual cortex: J. Physiol. (Lond.) 348:153–185.

Allman JM, Meizin F, McGuiness E (1985) Stimulus specific responses from beyond the classical receptive field: neurophysiological mechanisms for local-global comparisons in visual neurons. Annu. Rev. Neurosci. 5:407–430.

Amir Y, Harel M, Malach R (1993) Cortical hierarchy reflected in the organization of intrinsic connections in macaque monkey visual cortex. J. Comp. Neurol. 334:19–46.

Ben-Yishai R, Bar-Or RL, Sompolinsky H (1995) Theory of orientation tuning in visual cortex. Proc. Natl. Acad. Sci. USA 92:3844–3848.

Ben-Yishai R, Hansel D, Sompolinsky H (1997) Traveling waves and the processing of weakly tuned inputs in a cortical network module. J. Comput. Neurosci. 4: 57–77.

Blakemore C, Van Sluyters RC (1975) Innate and environmental factors in the development of the kitten's visual cortex. J. Physiol. 248:663–716.

Blasdel GG, Fitzpatrick D (1984) Physiological organization of layer 4 in macaque striate cortex. J. Neurosci. 4:880–95.

Bonds AB (1989) The role of inhibition in the specification of orientation selectivity of cells in the cat striate cortex. Vis. Neurosci. 2:41–55

Bosking WH, Zhang Y, Schofield B, Fitzpatrick D (1997) Orientation selectivity and the arrangement of horizontal connections in tree shrew striate cortex. J. Neurosci. 17:2112–2127.

Buisseret P, Imbert M (1976) Visual cortical cells: their developmental properties in normal and dark-reared kittens. J. Neurophysiol. 255:511–525.

Bullier J, Henry GH (1979) Laminar distribution of first order neurons and afferent terminals in cat striate cortex. J. Neurophysiol. 42:1271–1281.

Buxhoeveden DP, Casanova MF (2002) The minicolumn hypothesis in neuroscience. Brain 125:935–951.

Chapman B, Gödecke I, Bonhoeffer T (1999) Development of orientation preference in the mammalian visual cortex. J. Neurobiol. 41:18–24.

Chapman B, Stryker MP (1993) Development of orientation selectivity in ferret visual cortex and effects of deprivation. J. Neurosci. 13:5251–5262.

Chapman B, Stryker MP, Bonhoeffer T (1996) Development of orientation preference maps in ferret primary visual cortex. J. Neurosci. 16:6443–6453.

Chapman B, Zahs KR, Stryker MP (1991) Relation of cortical cell selectivity to alignment of receptive fields of the geniculocortical afferents that arborize within a single orientation column in ferret visual cortex. J. Neurosci. 11:1347–1358.

Chisum HJ, Mooser F, Fitzpatrick D (2003) Emergent properties of layer 2/3 neurons reflect the collinear arrangement of horizontal connections in tree shrew visual cortex. J. Neurosci. 23:2947–2960.

Crair MC, Gillespie DC, Stryker MP (1998) The role of visual experience in the development of columns in cat visual cortex. Science 279:566–570.

Çürüklü B, Lansner A (2002) An abstract model of a cortical hypercolumn, in: IEEE Proc., International Conference on Neural Information Processing 80–85.

Çürüklü B, Lansner A (2003) Quantitative assessment of the local and long-range horizontal connections within the striate cortex, in: IEEE Proc. Computational Intelligence, Robotics and Autonomous Systems.

Çürüklü B, Lansner A (2004) A Model of the Summation Pools within the Layer 4 (Area 17). The Annual Computational Neuroscience Meeting 2004, Baltimore, USA.

Das A (1996) Orientation in visual cortex: a simple mechanism emerges. Neuron 16:447–480.

Dean AF (1981) The relationship between response amplitude and contrast for cat striate cortical neurons. J. Physiol. 318:413–427.

DeAngelis GC, Freeman RD, Ohzawa I (1994)Length and width tuning of neurons in the cat's primary visual cortex. J. Neurophysiol. 71:347–374.

Derrington AM, Fuchs AF (1979) Spatial and temporal properties of X and Y cells in the cat lateral geniculate nucleus. J. Physiol. 293:347–364.

Durack JC, Katz LC (1996) Development of horizontal projections in layer 2/3 of ferret visual cortex. Cerebral Cortex 6:178–183.

Einstein G, Davis TL, Sterling P (1987) Pattern of lateral geniculate synapses on neuron somata in layer IV of the cat striate cortex. J. Comp. Neurol. 260:76–68.

Ferster D (1986) Orientation selectivity of synaptic potentials in neurons of cat primary visual cortex. J. Neurosci. 6:1284–1301.

Ferster D (1988) Spatially opponent excitation and inhibition in simple cells of the cat visual cortex, J. Neurosci., 8:1172–1180.

Ferster D (1990) X- and Y-mediated synaptic potentials in neurons of areas 17 and 18 of cat visual cortex. Vis Neurosci 4:115–133.

Ferster D, Chung S, Wheat H (1996) Orientation selectivity of thalamic input to simple cells of cat visual cortex. Nature 380:249–252.

Ferster D, Lindstrom S (1983) An intracellular analysis of geniculo-cortical connectivity in area 17 of the cat. J. Physiol. (Lond.) 342:181–215.

Ferster D, Miller KD (2000) Neural mechanisms of orientation selectivity in the visual cortex. Annual Reviews of Neurosci. 23:441–471.

Fitzpatrick D (1996) The functional organization of local circuits in visual cortex: insights from the study of tree shrew striate cortex. Cerebral Cortex 6:329–341.

Frégnac Y, Imbert M (1978) Early development of visual cortical cells in normal and dark-reared kittens: the relationship between orientation selectivity and ocular dominance. J. Physiol. 278:27–44.

Garey LJ, Powell TPS (1971) An experimental study of the termination of the lateral geniculo-cortical pathway in the cat and monkey. Proc. R. Soc. Lond. [Biol.] 179:41–63.

Gilbert CD, Wiesel TN (1983) Clustered intrinsic connections in cat visual cortex. J. Neurosci. 3:1116–1133.

Gilbert CD, Wiesel TN (1985) Intrinsic connectivity and receptive field properties in visual cortex. Vis. Res. 25:365–374.

Gödecke I, Kim DS, Bonhoeffer T, Singer W (1997) Development of orientation preference maps in area 18 of kitten visual cortex. Eur. J. Neurosci. 9:1754–1762.

Hawken M, Parker AJ (1984) Contrast sensitivity and orientation selectivity in lamina IV of the striate cortex of old world monkeys. Exp. Brain Res. 54:367–72.

Hirsch JA, Alonso J-M, Pillai C, Pierre C (2000) Simple and complex inhibitory cells in layer 4 of cat visual cortex. Soc. Neurosci. Abstr. 26:1083.

Hirsch JA, Martinez LM, Pillai C, Alonso J-M, Wang Q, Sommer FT (2003) Functionally distinct inhibitory neurons at the first stage of visual cortical processing. Nat. Neurosci. 6:1300–1308.

Holst A (1997) The use of a Bayesian neural network model for classification tasks. PhD Thesis Department of Numerical Analysis and Computing Science, Royal Institute of Science, Stockholm, Sweden, TRITA-NA-P9708.

Hornung JP, Garey LJ (1981) The thalamic projection to the cat visual cortex: ultrastructure of neurons identified by Golgi impregnation or retrograde horseradish peroxidase transport. Neuroscience 6:1053–1068.

Howell ER, Hess RF (1978) The functional area for summation to threshold for sinusoidal gratings. Vision Res., 18:369–374.

Hubel DH, Wiesel TN (1962) Receptive fields, binocular interaction and functional architecture in the cat's visual cortex, J. Physiol., 160:106–154.

Hubel DH, Wiesel TN (1963) Receptive fields of cells in striate cortex of very young, visually inexperienced kittens. J. Neurophysiol. 26:994–1002.

Hubel DH, Wiesel TN (1977) The functional architecture of the macaque visual cortex, The Ferrier lecture. Proc. Royal. Soc. B. 198:1–59.

Humphrey AL, Norton TT (1980) Topographic organization of the orientation column system in the striate cortex of the tree shrew (Tupaia glis). I. Microelectrode recording. J. Comp. Neurol. 192:531–547.

Jones JP, Palmer LA (1987) The two-dimensional spatial structure of simple cell receptive fields in cat striate cortex. J. Neurophysiol. 58:1187–1211.

Kaplan E, Shapley RM (1982) X and Y cells in the lateral geniculate nucleus of macaque monkey. J Physiol. London 330:125–143.

Kayser AS, Miller KD (2002) Opponent inhibition: a development model of layer 4 of the neocotical circuit. Neuron 33:131–142.

Kisvárday ZF, Tóth E, Rausch M, Eysel UT (1997) Orientation-specific relationship between populations of excitatory and inhibitory lateral connections in the visual cortex of the cat. Cerebral Cortex 7:605–618.

Krimer LS, Goldman-Rakic PS (2001) Prefrontal Microcircuits: Membrane properties and excitatory input of local, medium, wide arbor interneurons. J. Neurosci., 21:3788–3796.

Kritzer MF, Cowey A, Somogyi P (1992) Patterns of inter- and intralaminar GABAergic connections distinguish striate (V1) and extrastriate (V2, V4) visual cortices and their functionally specialized subdivisions in the Rhesus monkey. J Neurosci 12:4545–4564.

Lansner A, Ekeberg Ö (1987) An associative network solving the "4-bit adder problem". In: Caudill M, Butler C (editors). IEEE First International Conference on Neural Networks. Pp II–549.

Lansner A, Ekeberg Ö (1989) A one-layer feedback artificial neural network with a bayesian learning rule. Int. J. Neural Syst. 1:77–78.

Lansner A, Holst A (1996) A higher order bayesian neural network with spiking units. Int. J. Neural Syst. 7:115–128.

Lauritzen TZ, Miller KD (2003) Different roles for simple-cell and complex-cell inhibition in V1. J. Neurosci. 23:10201–10213.

LeVay S (1986) Synaptic organization of claustral and geniculate afferents to the primary visual cortex of the cat. J. Neurosci. 6:3564–3575.

LeVay S, Gilbert CD (1976) Laminar patterns of geniculocortical projections in the cat. Brain Res. 113:1–19.

Lund JS, Angelucci A, Bressloff PC (2003) Anatomical substrates for functional columns in macaque monkey primary visual cortex. Cerebral Cortex 12:15–24.

Orban GA Neuronal operation in the visual cortex. Berlin: Springer Verlag, 1984.

Maffei L, Fiorentini A, Bisti S (1973) Neural correlate of perceptual adaptation to gratings. Science 182:1036–1038.

Malach R, Amir Y, Harel M, Grinvald A (1993) Relationship between intrinsic connections and functional architecture revealed by optical imagining and in vivo targeted biocytin injections in primate striate cortex. Proc. Natl. Acad. Sci. USA 90:10496–10473.

Martin KAC (2002) Microcircuits in visual cortex. Current Opinion in Neurobiology 12:418–425.

Martin KAC, Whitteridge D (1984) Form, function and intracortical projections of spiny neurons in the striate visual cortex of the cat. J. Physiol. (Lond.) 353:463–504.

McDonald CT, Burkhalter A (1993) Organization of long-range inhibitory connections within rat visual cortex. J Neurosci 13:768–781.

McLaughin D, Shapley R, Shelley M, Wielaard DJ (2000) A neuronal network model of macaque primary visual cortex (V1): orientation selectivity and dynamics in the input layer 4Cα. Proc. Natl. Acad. Sci. USA 97:8087–8092.

Miller KD, Erwin E, Kayser A (1999) Is the development of orientation selectivity instructed by activity? J. Neurobiol. 41:44–57.

Morrone MC, Burr DC, Maffei L (1982) Functional implications of cross-orientation inhibition of cortical visual cells. I. Neurophysiological evidence. Proc. R. Soc.London Ser. B 216:335–54

Mountcastle VB (1957) Modality and topographic properties of single neurons of cat's somatic sensory cortex. J. Neurophysiol. 20:408–438.

Mountcastle VB (1978) An organizing principle for cerebral function. In: Edelman GM, Mountcastle VB (editors). The mindful brain. MIT Press 7–50.

Mountcastle VB (1997) The columnar organization of the neocortex. Brain 120:701–722.

Pei X, Vidyasagar TR, Volgushev M, Creutzfeldt OD (1994) Receptive field analysis and orientation selectivity of postsynaptic potentials of simple cells in cat visual cortex. J. Neurosci. 14:7130–7140.

Peters A, Payne BR (1993) Numerical relationships between geniculocortical afferents and pyramidal cell modules in cat primary visual cortex. Cereb. Cortex 3:69–78.

Polat U, Norcia AM (1998) Elongated physiological summation pools in the human visual cortex, Vision Res., 38:3735–3741.

Polat U, Sagi D (1993) Lateral interactions between spatial channels: Suppression and facilitation revealed by lateral masking experiments. Vision Res., 33:993–999.

Polat, U, Sagi, D (1994) The architecture of perceptual spatial interactions. Vision Res., 34:73–78.

Polat U, Sagi D (1994) Spatial interactions in human vision: From near to far via experience-dependent cascades of connections. Proceedings of the National Academy of Science USA, 91:1206–1209.

Polat U, Tyler CW (1999) What pattern the eye sees best, Vision Res., 37:887–895.

Powell TPS, Mountcastle VB (1959) Some aspects of the functional organization of the cortex of the postcentral gyrus of the monkey: a correlation of findings obtained in a single unit analysis with cytoarchitecture. Bull Johns Hopkins Hosp. 105:133–162.

Reid RC, Alonso JM (1995) Specificity of monosynaptic connections from thalamus to visual cortex. Nature 378:281–284.

Robson JG, Graham N (1981) Probability summation and regional variation in contrast sensitivity across the visual field. Vision Res., 21:409–418.

Rockland KS (1985) Anatomical organization of primary visual cortex (area 17) in the ferret. J. Comp. Neurol. 241:225–236.

Rockland KS, Lund JS (1982) Widespread periodic intrinsic connections in the tree shrew visual cortex. Science 215:1532–1534.

Rockland KS, Lund JS (1983) Intrinsic laminar lattice connections in primate visual cortex. J. Comp. Neurol. 216:303–318.

Roerig B, Chen B (2002) Relationships of local inhibitory and excitatory circuitry to orientation preference maps in ferret visual cortex. Cereb Cortex, 12:197–198.

Sandberg A (2003) Bayesian attractor neural networks of memory. PhD Thesis Department of Numerical Analysis and Computing Science, Royal Institute of Science, Stockholm, Sweden, TRITA-NA-0310.

Sandberg A, Lansner A, Petersson FM, Ekeberg Ö (2002) A Bayesian attractor network with incremental learning, Network: Computing in Neural Systems, 13:179–194.

Schmidt KE, Kim D-S, Singer W, Bonhoeffer T, Löwel S (1997) Functional specificity of long-range intrinsic and interhemisphic connections in the visual cortex of strabismic Cats. J. Neurosci. 17:5480–5492.

Somers D, Dragoi V, Sur M (2002) Orientation selectivity and its modulation by local and long-range connections in visual cortex. in: Payne BR, Peters A (ed.). The cat primary visual cortex. Academic Press.

Somers D, Nelson SB, Sur M (1995) An emergent model of orientation selectivity in cat visual cortical simple cells. J. Neurosci. 15:5448–5465.

Sompolinsky H, Shapley R (1997) New perspectives on the mechanisms for orientation selectivity. Current Opinion in Neurobiology 7:514–522.

Stratford KJ, Tarczy-Hornoch K, Martin KA, Bannister NJ, Jack JJ (1996) Excitatory synaptic inputs to spiny stellate cells in cat visual cortex. Nature 382:258–261.

Troyer TW, Krukowski AE, Miller KD (1998) Contrast-invariant orientation tuning in cat visual cortex: thalamocortical input tuning and correlation-based intracortical connectivity. J. Neurosci. 18:5908–5927.

Troyer TW, Krukowski AE, Miller KD (2002) LGN input to simple cells and contrast-invariant orientation tuning: an analysis, J. Neurophysiol., 87:2741–2752.

White LE, Coppola DM, Fitzpatrick D (2001) The contribution of sensory experience to the maturation of orientation selectivity in ferret visual cortex. Nature 411:1049–1052.

Wielaard DJ, Shelley M, McLaughin D, Shapley R (2001) How simple cells are made in a nonlinear network model of the visual cortex. J. Neurosci., 21:5203–5211.

Wiesel TN, Hubel DH (1974) Ordered arrangement of orientation columns in monkeys lacking visual experience. J. Comp. Neurol. 158:307–318.

Winfield DA, Powell TPS (1983) Laminar cell counts and geniculo-cortical boutons in area 17 of cat and monkey. Brain Res. 227:223–229.

Yousef T, Bonhoeffer T, Kim D-S, Eysel UT, Tóth E, Kisvárday ZF (1999) Orientation topography of layer 4 lateral networks revealed by optical imagining in cat visual cortex (area 18), E. J. of Neurosci., 11:4291–4308.

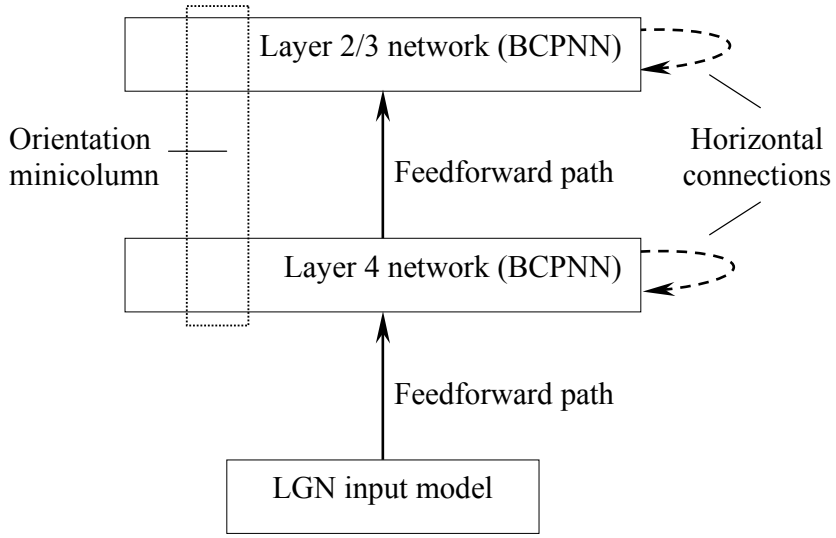

Figure 11.1. Illustration of the information flow within the V1 model. External input source of the layer 4 network is the LGN (solid line). Layer 2/3 units receive their external inputs from the layer 4 units (solid line). In both cortical layer models internal input is from other units in the same layer. This input is mediated by the horizontal connections (dashed lines). The feedforward path (solid lines), which consists of LGN → layer 4 → layer 2/3 is fixed, while the horizontal connections (see Figs. 11.2 and 11.6) are subject to change during the learning phase. Both the feedforward path and the horizontal connections are classified as excitatory. The horizontal connections target either other units directly (E→E), or through inhibitory interneurons (E→I), which are located in the near surrounding of the target units.

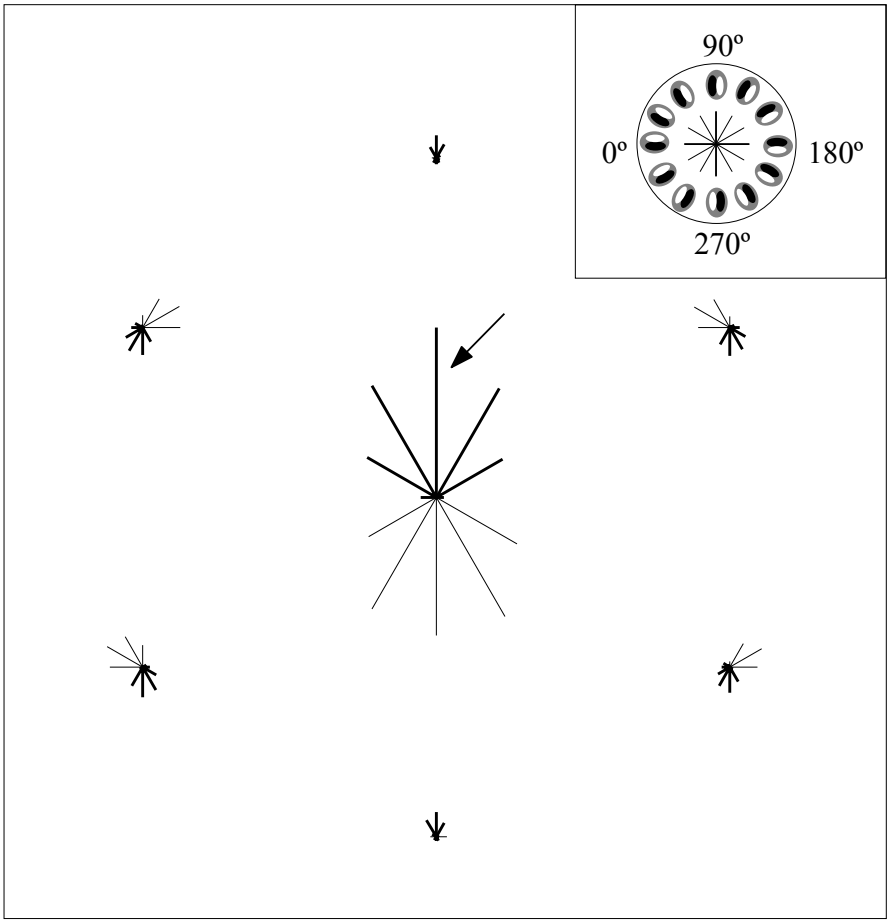

Figure 11.2. Illustration of the layer 4 reference unit's (marked with an arrow) isotropic summation pool consisting of seven hypercolumn-modules represented by as many polar graphs. The legend (top right) shows orientation preference as well as relative spatial phase of presynaptic units. Thick lines represent connections that target the reference unit directly (E→E), whereas thin lines correspond to projections to the inhibitory interneurons that are part of the reference unit (E→I). Since connection matrix is symmetric polar graphs can be interpreted as projections of the reference unit as well. The length of the lines (in polar graphs) is proportional to the strength of the corresponding connections.

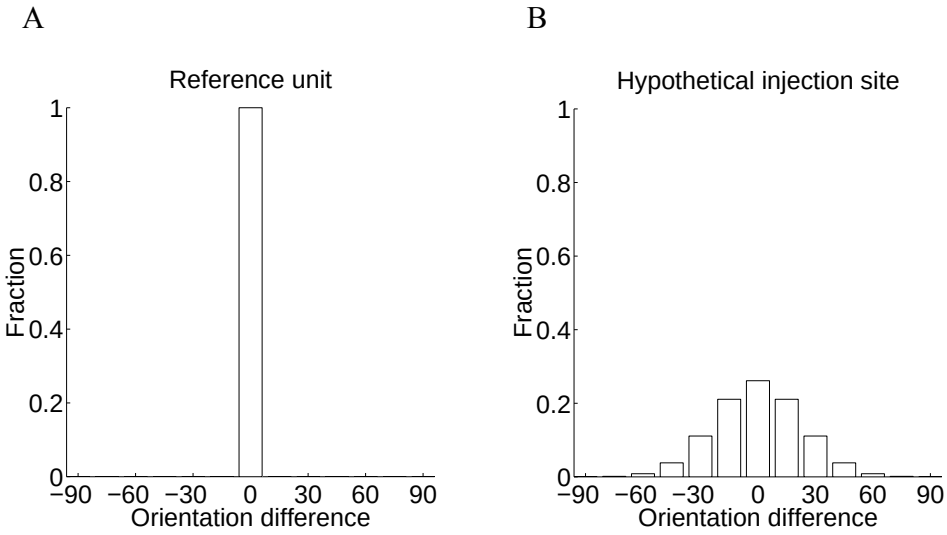

Figure 11.3. Distributions of the populations used in quantitative assessments. *A*. The population consists of the reference unit solely. *B*. The receiving population corresponds to an injection site, located at the reference unit.

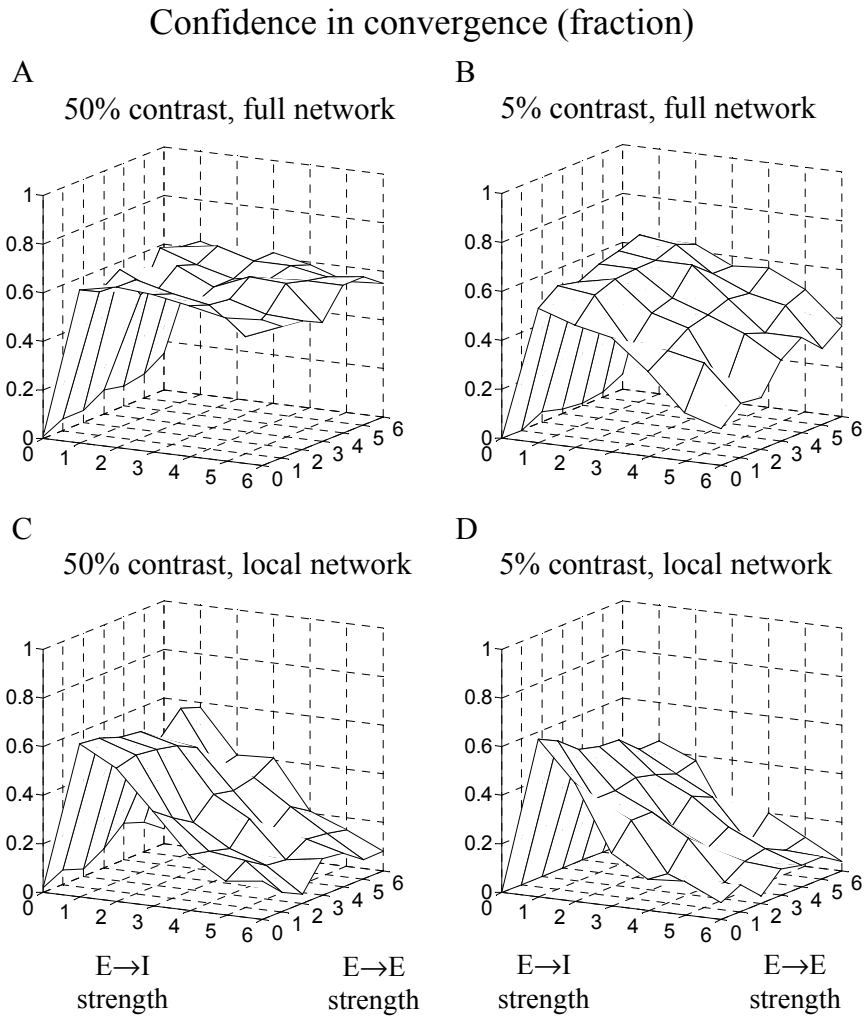

Figure 11.4. Confidence in convergence (defined as the number of correct detections divided by the number of trials) for the layer 4 reference unit (Fig. 11.2). *A–B*: Poor performance when E→E connections are absent, otherwise the full network can detect the contrast-edge. In low-contrast the network's performance decreases when excitation increases. This can be balanced by increase in inhibition though. Results are representative for the full network. *C–D*: The local network performs poorly independent of contrast. Inhibition does not seem to control excitation. Furthermore, ~25% of 200 trained layer 4 networks performed as this one, whereas in the rest OS was absent.

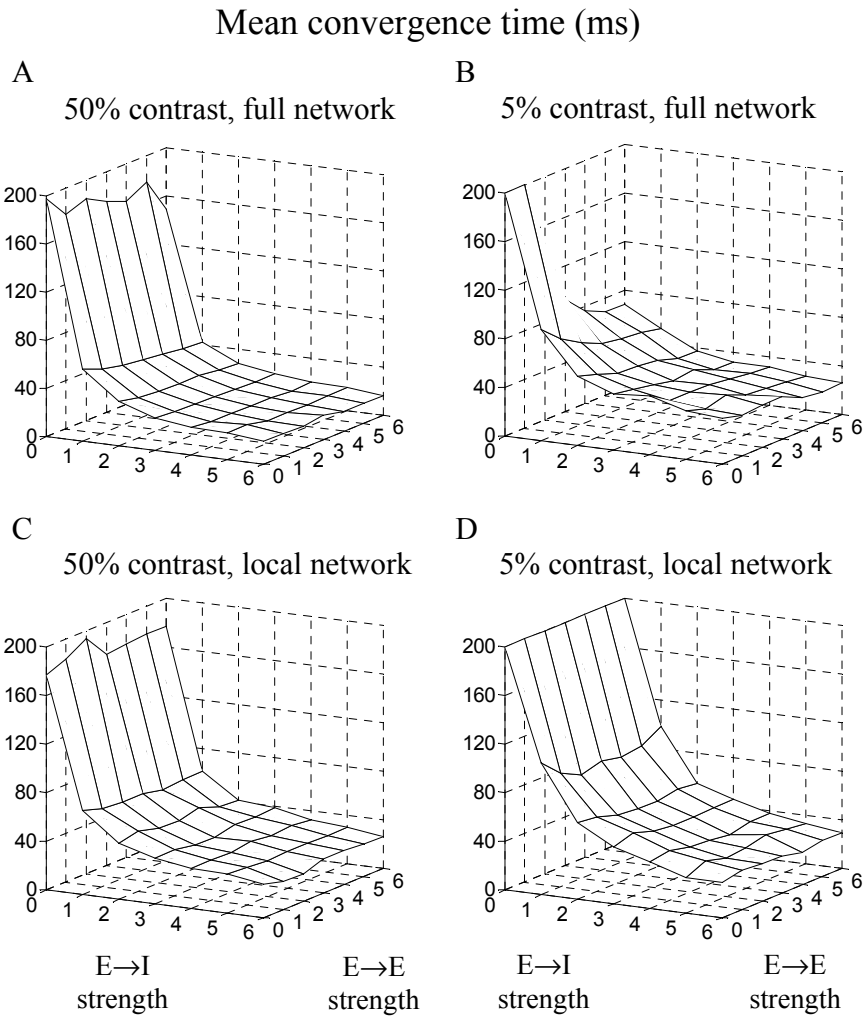

Figure 11.5. Mean convergence times of the reference unit calculated on correct detections (Fig. 11.4). In all cases both networks detect the stimulus faster when the excitatory strength is increased. Inhibitory strength does not influence convergence times. *A–B*: At E→E/I strengths = 1, convergence times are 53.5 ms (standard deviation = 9.3 ms) and 76.8 ms (standard deviation = 19.1 ms) for high- and low-contrast conditions, respectively, for the full network. Note that the network is somewhat slower in low-contrast. *C–D*: Similar results as in *A–B*, with convergence times 63.9 ms (standard deviation = 18.8 ms) and 93.2 ms (standard deviation = 23.7 ms). The local network converges slower than the full network.

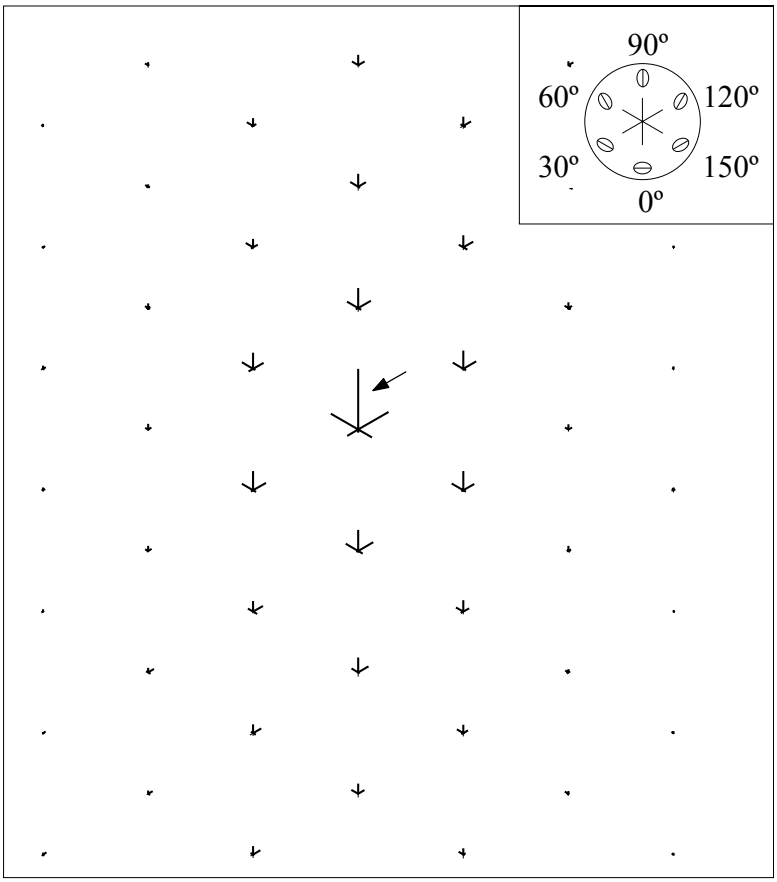

Figure 11.6. Illustration of the layer 2/3 reference unit's (marked with an arrow) elongated summation pool, which includes the whole layer 2/3 network. The legend (top right) shows the orientation preference of the presynaptic layer 2/3 units participating in the projections to the layer 2/3 reference unit. The summation pool is iso-orientation biased and antistrophic along the orientation axis of the layer 2/3 reference unit. Thick lines represent E→E connections. Note the absence of E→I connections. The length of the lines is proportional to the strength of the corresponding connection. Since connection matrix is symmetric E→E connections are reciprocal, and hence the figure can be interpreted as the projections of the layer 2/3 reference unit.

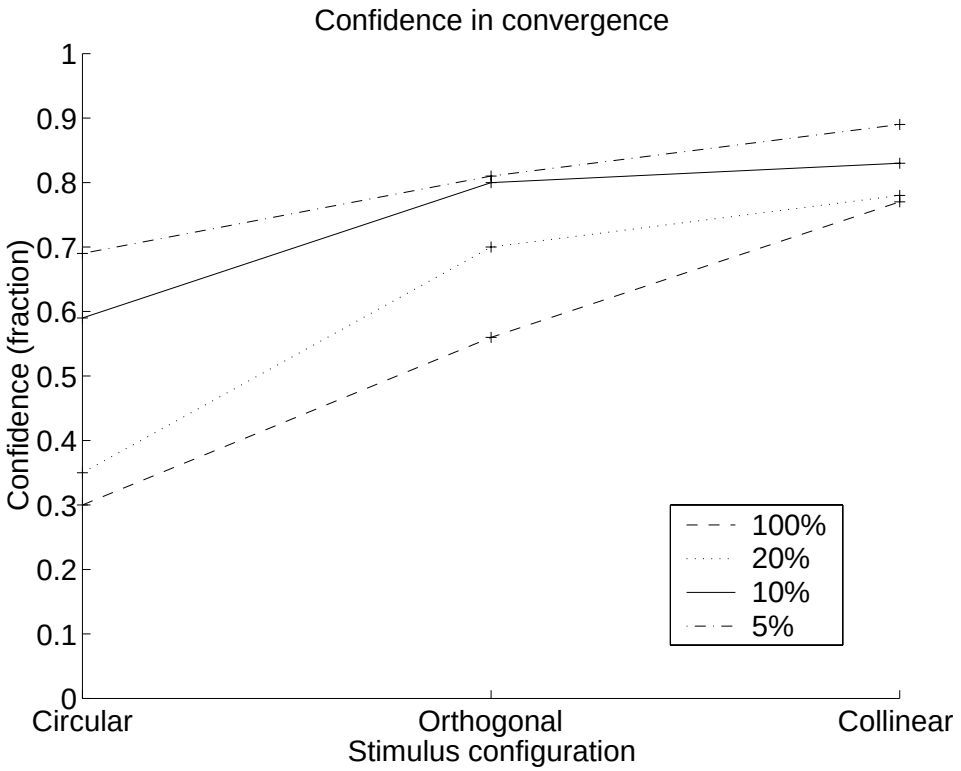

Figure 11.7. Confidence in convergence for the layer 2/3 reference unit (Fig. 11.6). The confidence is a function of both stimulus configuration and contrast. Network behavior is investigated on four contrast levels (5, 10, 20, and 100 %), and three stimulus configurations (circular, orthogonal and collinear configuration).

	Iso-orientation (%)	Oblique-orientation (%)	Cross-orientation (%)
E→E (local)	49.2	34.0	16.8
(long-range)	50.4	32.8	16.8
E→I (local)	47.1	38.0	14.9
(long-range)	23.4	29.4	47.2
Total (local)	48.2	36.0	15.8
(long-range)	38.2	31.3	30.5

Table 11.1. Distribution of the horizontal connections that target the reference unit located in layer 4 (Fig. 11.6*A*). The projections are either direct, i.e. they target the reference unit though E→E connections, or indirect. In the latter case connections target the local interneurons through E→I connections. The distributions are calculated based on the sum of the log weights for each category. Local connections are within the same hypercolumn-module, whereas long-range connections travel between two hypercolumn-modules. The projections are classified as from iso-, oblique- and cross-orientation domains relative the reference unit.

	Iso-orientation (%)	Oblique-orientation (%)	Cross-orientation (%)
E→E (local)	40.8	33.3	25.9
(long-range)	40.6	33.2	26.2
E→I (local)	40.4	34.5	25.1
(long-range)	27.1	32.6	40.3
Total (local)	40.6	34.0	25.4
(long-range)	34.0	33.0	33.0

Table 11.2. Distribution of the horizontal connections that target the injection site located in layer 4 (Fig. 11.6*B*). These projections are either direct, i.e. they target the reference unit though E→E connections, or indirect. In the latter case connections target the local interneurons through E→I connections. The distributions are calculated based on the sum of the log weights for each category. Local connections are within the same hypercolumn-module, whereas long-range connections travel between two hypercolumn-modules. The projections are classified as from iso-, oblique- and cross-orientation domains relative the reference unit.

	Iso-orientation (%)	**Oblique-orientation (%)**	**Cross-orientation (%)**
E→E (local)	55.0	30.0	15.0
(long-range)	53.5	30.5	16.0

Table 11.3. Distribution of the E→E connections that target the reference unit located in layer 2/3 (Fig. 11.6*A*). The distributions are calculated based on the sum of the log weights for each category. Local connections are within the same hypercolumn-module, whereas long-range connections travel between two hypercolumn-modules. The projections are classified as from iso-, oblique- and cross-orientation domains relative the reference unit.

	Iso-orientation (%)	Oblique-orientation (%)	Cross-orientation (%)
E→E (local)	51.3	32.7	16.0
(long-range)	50.0	33.3	16.7

Table 11.4. Distribution of the E→E connections that target the injection site located in layer 2/3 (Fig. 11.6*B*). The distributions are calculated based on the sum of the log weights for each category. Local connections are within the same hypercolumn-module, whereas long-range connections travel between two hypercolumn-modules. The projections are classified as from iso-, oblique- and cross-orientation domains relative the reference unit.

	$1/\lambda_{st}$ (c/deg)	γ_x/σ_{st} (deg)	γ_y/σ_{st} (deg)
Circular	1	1/6	1/6
Orthogonal	1	∞^{-1}	1/6
Collinear	1	1/6	∞^{-1}

Table 11.5. Parameter settings for the Gabor stimuli used in the configuration-specific facilitation study (see Section 11.5.1). Circularly configured stimulus is isotropic. Orthogonal configuration is when the stimulus is elongated along the horizontal axis. Collinear configuration is equal to a vertical contrast-edge (similar to the stimuli used during the training). Note that spatial frequency and orientation of the stimuli are same in all three cases.